Optically transparent and circularly polarized patch antenna for k-band applications

Q. H. Dao
T. J. Cherogony
B. Geck

Optically Transparent and Circularly Polarized Patch Antenna for K-Band Applications

Q. H. Dao, T. J. Cherogony, B. Geck

Institut für Hochfrequenztechnik und Funksysteme

Leibniz Universität Hannover

Hannover, Germany

dao@hft.uni-hannover.de

Abstract—**This contribution presents an optically transparent and circularly polarized patch antenna to be integrated on a solar cell. The whole configuration is suitable to be use in a wireless sensor node acting as a communication interface and a power source. The antenna consisting of grid lines is studied concerning the impedance behavior due to the applied mesh. A single fed truncated corners meshed patch antenna with meshed ground plane on quartz glass is investigated. This structure with an overall transparency of 92 % has similar antenna properties to the opaque counterpart. Additionally, the alignment errors between both meshed layers possibly caused by the fabrication process is addressed concerning the axial ratio. A prototype is realized and measured to verify the simulation results.**

Keywords—optically transparent antenna; meshed patch antenna; circular polarization; k-band

Fig. 1: Explosion view of the proposed design concept of an optically transparent and circularly polarized patch antenna capable of integrated on a solar cell

I. Introduction

Today, the Internet of Things (IoT) is one of the important innovation drivers in the field of economy and society. Intelligent and networked devices can be found in industrial environment as well as in everyday life. Some applications are for example connected cars, wearables, smart homes or industry 4.0. In the field of production engineering it is desirable to use wireless sensor nodes (WSN) within a wireless sensor network for an exchange of information such as ID number or sensor data. Additionally, during the life cycle of a component it is important to know its current status [1]. For this reason the WSN should be designed to ensure a long life time. In this case a battery is not suitable because of the possible high energy consumption of the utilized application. Therefore, the battery has to be replaced after days, months or just a few years. Using an energy harvesting concept such as a solar cell the life time of the WSN is not limited. Another important aspect is the size which should be kept as small as possible. Thus, we pursue an approach of integrating the optically transparent antenna on a solar cell [2] [3]. This concept is illustrated in Fig. 1. For the realization it is necessary to use an optically transparent substrate and the antenna structure itself has to have a high optical transparency too. Using transparent conducting oxides (TCOs) as conductive layer is one possible way but due to its high resistivity it leads to a poor antenna efficiency [4]. An alternative way of obtaining high optical transparency and high antenna efficiency simultaneously is designing the microstrip antenna by means of grid lines. It was shown in [2] that linear polarized patch antennas consisting of a grid have properties comparable to conventional patch structures. In this contribution the antenna is designed in a manner having the capability of transmitting circular polarization waves to ensure a proper communication link between wireless sensor nodes regardless of the orientation of the antenna. Applying an optically transparent and circularly polarized patch antenna on a solar cell is an efficient way to realize a highly integrated wireless sensor node.

This paper is structured as follows. First, an antenna concept will be introduced suitable to generate circular polarization. Afterwards, the opaque layout is meshed to achieve optical transparency and the changes of impedance are studied. In section III a meshed patch antenna designed on quartz glass is presented. The influences on the antenna properties caused by possible misalignment due to the fabrication process is studied. The last section deals with the verification of the simulation results.

II. Circularly Polarized Patch Antennas

There are many possibilities to develop circularly polarized (CP) patch antennas. One way is exciting the patch by two feeds with a phase difference of 90° at adjacent edges of the patch. The other possibility is using a single feed to generate two orthogonal modes. Therefore, a perturbation segment such as a slot or other truncated segment methods can be utilized [5]. In this
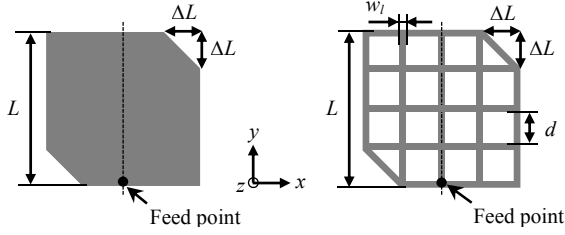
(a) Conventional structure   (b) Meshed structure with five horizontal and vertical grid lines

Fig. 2: Geometry of the RHCP singly fed truncated corners square patch antenna
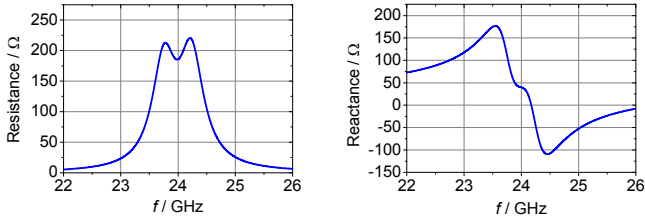
Fig. 3: Impedance graph of a conventional CP truncated corners patch antenna fed at the edge

contribution single fed truncated corners patch antennas (see Fig. 2) are investigated because of its simple feeding method. Hereby, quartz glass is used as carrier material to meet the requirement of optical transparency. It has a thickness of 0.2 mm and the dielectric constant is $\epsilon_r' = 3.81$ and $\tan \delta = 0.0004$ at 24 GHz which is determined by a resonator measurement method. The conductive layers are assigned as copper with a thickness of 1 μm since the intended RF sputtered metal coating layers are in this range of thickness. The simulations are carried out using Ansys HFSS 2015.

A. Conventional Structure

Fig. 2a shows a square patch structure with an edge length L truncated at the lower left and upper right corner to achieve right hand circular polarization (RHCP). A precise ratio of patch edge length L and cut size ΔL leads to a minimum axial ratio. The feed point can be varied along the center line for impedance matching. A typical simulated impedance curve for such a structure is depicted in Fig. 3. In this case the antenna is fed at the edge using a lumped port. At the resonance frequency of 24 GHz the resistance is 185 Ω and the reactance is 39.7 Ω.

B. Meshed Structure

To get an optically transparent antenna the opaque structure can be designed as meshed structure. Fig. 2b shows an example of an antenna configuration consisting of five horizontal and five vertical grid lines specified with a width of w_l. All grid lines are separated by the distance d. In the following the impedance behavior of such a meshed antenna is studied. According to [2] the grid line width and the distance d should be as small as possible to achieve a high optical transparency and simultaneously antenna properties comparable to conventional patch antenna. Thus, the square patch is divided into eleven

TABLE I: Impedance values at resonance frequency (24 GHz, minimum AR, fed at edge) of the structures with meshed patch and opaque ground plane

AUT	w_l / μm	d / m	Re{Z} / Ω	Im{Z} / Ω
Nr. 1	100	$\lambda_r/65.4$	147	51
Nr. 2	50	$\lambda_r/51.9$	189	38
Nr. 3	10	$\lambda_r/45.2$	197	40

TABLE II: Impedance values at resonance frequency (24 GHz, minimum AR, fed at edge) of the structures with meshed patch and meshed ground plane

AUT	w_l / μm	d / m	Re{Z} / Ω	Im{Z} / Ω
Nr. 4	100	$\lambda_r/66.7$	188	38
Nr. 5	50	$\lambda_r/53.5$	198	42
Nr. 6	10	$\lambda_r/46.6$	172	54

horizontal and eleven vertical lines. Afterwards, the line width is set to 100, 50 and 10 μm resulting in three different antennas under test (AUT 1-3). The corresponding distance values d (relative to the resonance wavelength λ_r in free space) as well as the impedance values are listed in Table I. Hereby, the impedance values are evaluated at the resonance frequency of 24 GHz and an axial ratio lower than 2 dB. The feed point is located at the edge. With smaller line width the distance gets higher and the resistance value increases while the reactance changes in the range of ± 7 Ω. To design an optically transparent antenna the ground plane has to be meshed too. Table II summarizes the impedance values of the AUT number 4 to 6 consisting of a meshed patch and a meshed ground plane. In comparison with AUT number 1 to 3 it can be noted that a gridded ground plane also causes a variation of resistance and reactance values.

III. OPTICALLY TRANSPARENT ANTENNA

Fig. 4 shows the layout of an optically transparent and RHCP antenna. The square patch consists of eleven horizontal and eleven vertical grid lines with a line width $w_l = 20$ μm and a spacing of $d = \lambda_r/48.1$. The grid line width of the ground plane and the grid spacing is set to 10 μm and $\lambda_r/46.5$, respectively. These values are a compromise between antenna performance and optical transparency. Furthermore, both the patch (colored area) and the ground plane (grey area) are aligned in a way to get a high transparency. The geometry dimensions of the whole antenna are marked in Fig. 4. As can be seen from this layout the antenna is fed at the edge using a microstrip line consisting of three sections of the length L_F, L_T and L_{MS}. The section touching the antenna has a line width of 80 μm. The wave port of the simulator is connected to the 50 Ω line labelled with w_{MS}. The microstrip lines are designed for an optimal impedance matching. Furthermore, the grid spacing of the microstrip lines and its ground plane is kept small to minimize insertion losses
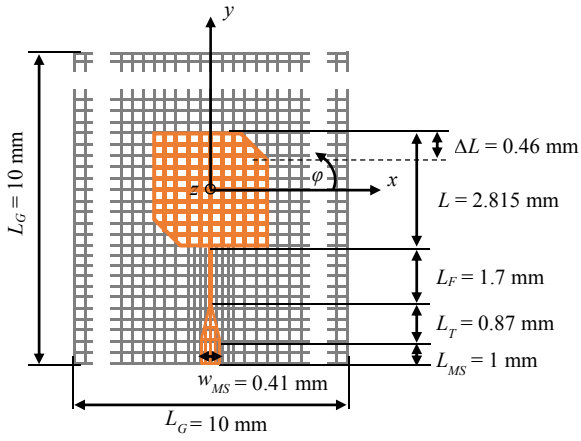
Fig. 4: Simulation model of the transparent and RHCP antenna
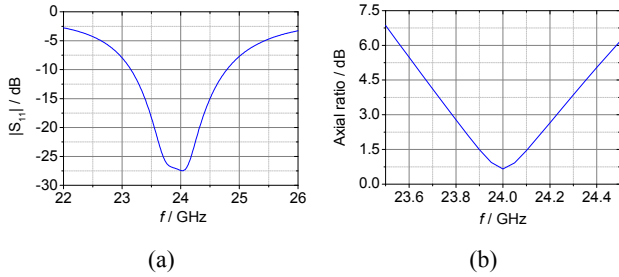
Fig. 5: Simulated reflection coefficient and axial ratio of the optically transparent antenna with a transparency of 92 %

of the incident wave. The whole antenna has a transparency of roughly 92 % calculated by the ratio between the non-metal area and the total area.

The optimized simulation results are depicted in Fig. 5. The input reflection coefficient $|S_{11}| = $ -27 dB at 24 GHz and the bandwidth ($|S_{11}| \leq $ -10 dB) is 6.7 %. The axial ratio over the frequency is plotted in Fig. 5b. The minimum value of 0.6 dB can be obtained at 24 GHz. The axial ratio bandwidth (axial ratio $\leq$ 3 dB) is 1.87 %. This meshed antenna has a simulated realized gain value of 4 dBi in the main direction ($\vartheta = \varphi = 0°$) while the gain value for a correspondent non-meshed patch antenna is 6.2 dBi. Apart from the lower antenna gain the advantages of using grid lines are that broader operating bandwidth and axial ratio bandwidth can be achieved compared to the opaque counterpart.

A. Misalignment

Due to the very thin grid lines of both layers which should be precisely aligned to each other during the fabrication process, a small misalignment between the top and bottom side leads to a degradation in optical transparency. Furthermore, an influence on the antenna performance can be expected [6]. Thus, the effects on antenna properties are studied in the following. Alignment errors can occur due to a translation in x-direction, y-direction, a rotation of a certain angle or even a combination of all of this. Fig. 6 depicts three different configurations (geometry dimensions correspond to Fig. 4) which are investigated. Hereby, one layer is fixed and the position of the second layer is varied. The alignment errors caused by a translation are
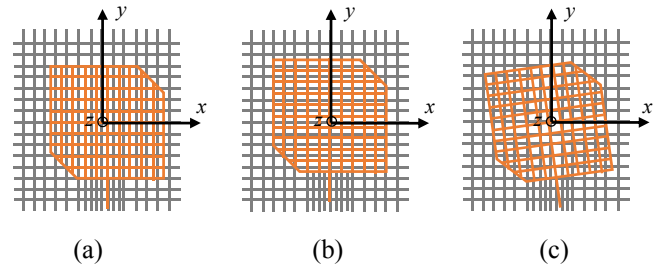
Fig. 6: Misalignment between top and bottom layer (a) Translation in x-direction (b) Translation in y-direction (c) Rotation around origin

(a)

(b)
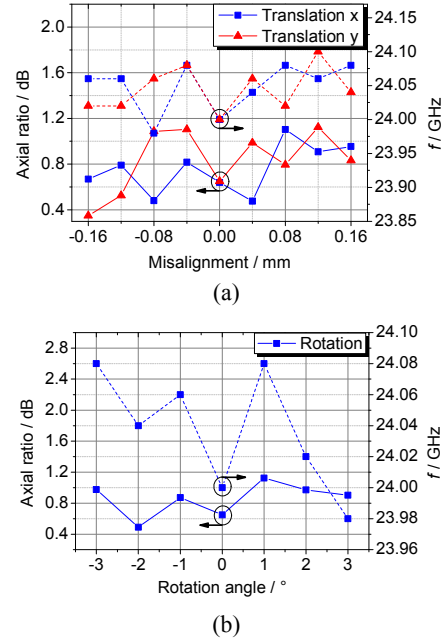
Fig. 7: Simulation results of the axial ratio and the frequency shift (shift of the frequency position showing minimum axial ratio value) due to misalignment concerning translation and rotation

illustrated in Fig. 6a and Fig. 6b. The simulation results of the respective minimum axial ratio and the corresponding frequency value are depicted in Fig. 7a. Misalignments by means of translation of ±0.16 mm (correspond to ±68 % of the grid space of $d = \lambda_r/46.5$) are considered. For both configurations a maximum deviation of 0.5 dB of axial ratio and a maximum frequency shift of 100 MHz are observed. Errors due to a rotation of ±3° between both layers (cf. Fig. 6c) causes a change of the axial ratio value of 0.5 dB and a frequency shift of 80 MHz. These results are plotted in Fig. 7b. It can concluded that a slight misalignment during the fabrication process will not influence the antenna performances dramatically.

IV. REALIZATION AND VERIFICATION

Due to the small line width and the associated complex manufacturing process the production of the investigated antenna in section III is not yet fabricated. Instead of that an alternative antenna layout consisting of eleven horizontal and eleven vertical grid lines is designed on the opaque high

(a) Top side   (b) Bottom side
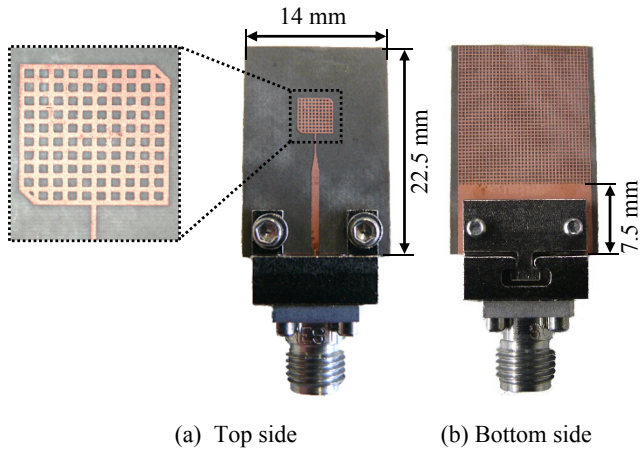
Fig. 8: Pictures of the realized optically transparent and circularly polarized patch antenna (opaque Rogers RT/duroid 5880 laminate)

TABLE III: Geometry dimensions of the realized antenna

Dimensions	L	ΔL	L_F	L_T	L_{MS}	w_{MS}
mm	3.75	0.39	2	2.12	9	0.77

frequency laminate RT/duroid 5880. The used laminate has a thickness of 0.254 mm. Because of the limitations of the used etching process the line width w_l of the patch as well as the grid lines of the meshed ground plane is set to 100 µm. Thus, the grid space is $d = \lambda_r/47.1$. Pictures of the realized patch antenna are depicted in Fig. 8. The dimensions of this antenna according to the layout in Fig. 4 are listed in Table III. The length of the microstrip line L_{MS} is designed in a way to meet both the mechanical specifications of the end launch connector and the requirements of the TRL calibration process applying to the measurement procedure. For this purpose, a part of the ground plane of the microstrip section L_{MS} is designed as opaque up to the calibration reference plane

The simulation and measurement results of the prototype are depicted in Fig. 9. The blue curve (marked with triangles) in Fig. 9a represents the simulated input reflection coefficient and the red curve (marked with squares) is the measurement. A slight shift of the resonance frequency of 94 MHz corresponding to 0.4 % can be observed. This frequency shift can also be noticed at the curve of the axial ratio which is depicted in Fig. 9b. In this case a deviation of 1.6 dB can be determined. The minimum simulated and measured axial ratio value is 1.1 dB and 2.7 dB, respectively. This meshed antenna has a maximum realized gain of 5.9 dBi (measured) at the main direction ($\vartheta = \varphi = 0°$) which deviates from the simulation value by 1.2 dB.

V. CONCLUSION

This contribution presents the approach of a highly transparent patch antenna with right hand circular polarization. Section II shows the investigation of changes in impedance values caused by meshing the patch antenna. An optically

(a) Reflection coefficient   (b) Axial ratio
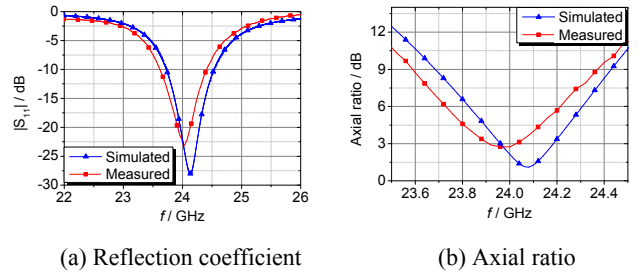
Fig. 9: Simulated and measured reflection coefficient and axial ratio of the realized prototype

transparent antenna with truncated corners feeding by means of a single microstrip line is studied. The proposed antenna has an optical transparency of 92 %, an input reflection coefficient of -27 dB and a minimum axial ratio of 0.6 dB at 24 GHz as well as a simulated realized gain value of 4 dBi in the main direction. By using grid lines broader operating bandwidth and axial ratio bandwidth are achieved. Possible alignment errors of the two-layer antenna during the fabrication process that may lead to influences on the antenna properties are discussed. It can be observed that a change of axial ratio less than 0.5 dB and the optimal operating frequency is shifted by ±0.2 %. Due to the high technological efforts the proposed antenna is not yet produced. Instead an alternative antenna is designed and fabricated on an opaque laminate to verify the simulation results. This prototype is evaluated in an anechoic chamber and it shows a maximum realized gain value of 5.9 dBi and a minimal axial ratio of 2.7 dB. All in all, a good agreement between simulation and measurement is achieved.

REFERENCES

[1] J. Meyer, Q. H. Dao, and B. Geck, "24 GHz rfid communication system for product lifecycle applications," in *2nd International Conference on System-Integrated Intelligence: New Challenges for Product and Production Engineering (SysInt)*, 2014.

[2] Q. H. Dao, R. Braun, and B. Geck, "Design and investigation of meshed patch antennas for applications at 24 GHz," in 45th European Microwave Conference (EuMC) 2015.

[3] T. Yasin, and R. Baktur, "Circularly polarized meshed patch antenna for small satellite application," *Antenna and Wireless Propagation Letters, IEEE, vol. 12, pp. 1057-1060, 2013*.

[4] T. Yasin, R. Baktur, and C. Furse, "A comparative study on two types of transparent patch antennas," in *General Assembly and Scientific Symposium, 2011 XXXth URSI*, Aug 2011, pp. 1-4.

[5] C. Sharma, and K.C. Gupta, "Analysis and optimized design of single feed circularly polarized microstrip antennas," *IEEE Transactions on Antennas and Propagation*, vol. AP-32, no. 6, pp. 949-955, 1983.

[6] J. Hautcoeur, L. Talbi, K. Hettak, and M. Nedil, "60 GHz optically transparent microstrip antenna made of meshed AuGl material," *IET Microw. Antennas Propag.*, vol. 8, Iss. 13, pp. 1091-1096, 2